HAL
open science

The local environment orchestrates mucosal decidual macrophage differentiation and substantially inhibits HIV-1 replication.

E El Costa, F Quillay, E Marlin, F Cannou, E Duriez, F Benjelloun, Claire de Truchis, F Rahmati, F Ighil, Françoise Barré-Sinoussi, et al.

To cite this version:

E El Costa, F Quillay, E Marlin, F Cannou, E Duriez, et al.. The local environment orchestrates mucosal decidual macrophage differentiation and substantially inhibits HIV-1 replication.. Mucosal Immunology, 2016, 9 (3), pp.634-46. 10.1038/mi.2015.87 . pasteur-01453433

HAL Id: pasteur-01453433

https://pasteur.hal.science/pasteur-01453433v1

Submitted on 13 Feb 2017

HAL is a multi-disciplinary open access archive for the deposit and dissemination of scientific research documents, whether they are published or not. The documents may come from teaching and research institutions in France or abroad, or from public or private research centers.

L'archive ouverte pluridisciplinaire **HAL**, est destinée au dépôt et à la diffusion de documents scientifiques de niveau recherche, publiés ou non, émanant des établissements d'enseignement et de recherche français ou étrangers, des laboratoires publics ou privés.

Distributed under a Creative Commons Attribution - NonCommercial - NoDerivatives 4.0 International License

The local environment orchestrates mucosal decidual macrophage differentiation and substantially inhibits HIV-1 replication

H El Costa[1], H Quillay[1,2], R Marlin[3,4,5,6], C Cannou[1], M Duriez[7], F Benjelloun[1], C de Truchis[8], M Rahmati[9], J Ighil[9], F Barré-Sinoussi[1], M T Nugeyre[1], E Menu[1,3,4,5,*]

[1]Institut Pasteur, Regulation of Retroviral Infection Unit, Paris, France
[2]Université Paris Diderot, Sorbonne Paris Cité, Cellule Pasteur, Paris, France
[3]Université Paris Sud, UMR 1184, France
[4]CEA, DSV/iMETI, Division of Immuno-Virology, IDMIT, France
[5]Inserm, U1184, Center for immunology of viral infections and autoimmune diseases, France
[6]Vaccine Research Institute (VRI), Créteil, France
[7]Sorbonne Universités, UPMC Univ Paris 06, INSERM U1135, Centre d'Immunologie et des Maladies Infectieuses (CIMI), Persistent Viral Infections (PVI) Team, Paris, France
[8]Gynecology-Obstetrics Service, A. Béclère Hospital, AP-HP, Clamart, France
[9]Gynecology-Obstetrics Service, Pitié Salpetrière Hospital AP-HP, Paris, France.

* Correspondence : E Menu, elisabeth.menu@pasteur.fr

Abstract

Macrophages from the *decidua basalis* (dM), the main uterine mucosa during pregnancy, are weakly permissive to HIV-1 infection. Here we investigated the mechanisms underlying this natural control. We show, by using freshly purified decidual macrophages and *ex vivo* human decidual explants, that the local decidual environment influences dM differentiation and naturally protects these cells from HIV-1 infection. IFN-γ, present in the decidual tissue, contributes to maintenance of the dM phenotype and restricts HIV-1 infection by mechanisms involving the cyclin-dependent kinase inhibitor p21Cip1/Waf1. We also found that activation of Toll-like receptors 7 and 8 expressed by dM reinforces the low permissivity of dM to HIV-1 by restricting viral replication and inducing secretion of cytokines in the decidual environment, including IFN-γ, that shape dM plasticity. A major challenge for HIV-1 eradication is to control infection of tissue-resident macrophages in the female reproductive tract. Our findings provide clues to the development of novel strategies to prevent HIV-1 macrophage infection.

Introduction

The *decidua basalis*, the main uterine mucosa during pregnancy, is a model for studying natural protection against HIV-1 mucosal infection. Indeed, maternofetal HIV-1 transmission is rare during the first trimester, and HIV-1 dissemination appears to be tightly controlled at the maternofetal interface [1]. Macrophages that reside in decidual tissue (dM) are fully differentiated. They are the main targets of CCR5-tropic HIV-1 but are less permissive to HIV-1 infection than their peripheral blood counterparts [2].

The *decidua basalis* is characterized by a specific pro/anti-inflammatory cytokine balance required to support fetal development. These cytokines maintain a state of local immune tolerance to the semi-allogeneic fetus and probably ensure host defenses against pathogens [3].

Pro- and anti-inflammatory cytokines trigger peripheral monocyte derived macrophage (MDM) differentiation into opposing programs. This polarization gives rise to two major macrophage phenotypes, designated M1 (classic) and M2 (alternative). M1 macrophages generated in response to cytokines such as IFN-γ and TNF-α, produce pro-inflammatory cytokines such as IL-12 and TNF-α and mediate resistance to pathogens. They express the transcription factor IRF5[4], the costimulatory molecules CD80 and CD86, and the FCγ receptor I CD64 [5,6]. M2 macrophages, generated in response to cytokines such as IL-10, produce anti-inflammatory cytokines (especially IL-10 and IL1-RA) and promote tissue remodeling. The surface-marker expression profile of M2 macrophages includes the scavenger receptor CD163 and the mannose receptor CD206 [5,6]. This MDM plasticity is linked to HIV-1 susceptibility [7].

62 Decidual macrophages have an M2-like phenotype and show features of pro-
63 inflammatory and tolerogenic macrophages, simultaneously expressing M1 (CD64,
64 CD80, CD86) and M2 markers (CD163, CD206) [2,8].

65 Another hallmark of the *decidua basalis* is the abundance of decidual natural killer
66 cells (dNK). The dNK cells secrete large amounts of IFN-γ and TNF-α and are
67 involved in the control of fetal cell invasion, initiation of endometrial vasculature.
68 These cells may limit also the spreading of viral infection to fetal tissues by
69 controlling intrauterine infection by hCMV [9] and HIV-1 (Quillay et al., manuscript
70 under revision).

71 dM and dNK cells express innate receptors, such as toll-like receptors 7 and 8
72 (TLR7/8), that sense HIV-1 sequences and are involved in mediating immune
73 activation following HIV-1 infection [3,10]. We have shown that, upon TLR7/8 activation,
74 dM and dNK cells secrete large amounts of cytokines [3]. TLR7/8 activation inhibits
75 HIV-1 replication in monocytes and MDM [11-14]. In addition, TLR7/8 may influence
76 macrophage polarization, either by activating signaling pathways or by inducing the
77 secretion of cytokines associated with macrophage polarization in the
78 microenvironment [3,14-16].

79 The aim of this work was to determine why dM are weakly permissive to HIV-1
80 infection during the first trimester of pregnancy, with a view to the development of
81 novel strategies for eradicating macrophage infection. We postulated that the
82 decidual environment must contain factors that shape dM plasticity and susceptibility
83 to HIV-1 infection, and that TLR7/8, if activated, can reinforce this low dM
84 permissivity by modulating the local environment and blocking HIV-1 replication.

Results

dM in culture undergo dynamic changes toward a more M2 profile and become more permissive to HIV-1 infection

To address whether the local decidual environment influences the susceptibility of dM to HIV-1 infection, dM were isolated and challenged with VSV-G pseudotyped HIV-1 (HIV-1/VSV-G), immediately after purification (day 0) or after 3 or 7 days of culture in cytokine-free medium. HIV-1 replication was monitored by measuring luciferase activity. Surprisingly, we found that freshly purified dM had very low permissivity to HIV-1/VSV-G but became more susceptible with time in culture (Figure 1a). Similar results were obtained when freshly purified dM and cultured dM were challenged with CCR5-using macrophage-tropic HIV-1_{BaL}, as shown by p24 Ag measurement (Figure 1b).

To explain these results, we monitored the surface expression of several macrophage markers by flow cytometry. Expression of M2 markers (CD163, CD206) increased in culture (Figures 2a and 2b), whereas expression of M1 markers (CD64, CD80, CD86) remained unchanged (Supplementary figure S1). We then analyzed HIV-1 receptor and co-receptor expression (CD4, CCR5 and DC-SIGN) and found that only CCR5 expression increased significantly over time (Figure 2c). Early after purification, these cells consisted of approximately equal numbers of spindle-shaped fibroblastoid cells and large flat-round cells (Supplementary figure S2a, left panel), whereas round-shaped cells gradually became predominant in culture (Supplementary figure S2a, right panel). This suggested that dM polarization switched towards a more M2 profile in culture. To confirm this, we used western blot to analyze the expression of the M1 transcription factor (IRF5) involved in the M2 to M1 switch. In keeping with our previous observations, IRF5 expression was

111 decreased gradually in culture (Figure 2d). Analysis of cytokine secretion showed
112 that dM maintained their secretion of M2 cytokines (IL-1RA and IL-10) over time
113 (Figure 2e).

114 Together, these results indicate that dM isolated from their local environment
115 acquire more M2 features and that this switch is accompanied by an increase in
116 susceptibility to HIV-1 infection.

117

118 **IFN-γ participates in dM differentiation and in resistance to HIV-1 infection**

119 The next step was to identify the decidual environmental factor(s) that,when
120 lacking in culture, trigger the dM polarization switch and enhance susceptibility to
121 HIV-1 infection. IFN-γ, present in the decidua, is one of the most potent stimuli of
122 endogenous M1 macrophage activation and play a crucial role in immune responses
123 against pathogens and in tumour immunosurveillance [17]. We thus investigated
124 whether IFN-γ affect dM plasticity and susceptibility to HIV-1 infection.

125 IFN-γ treatment immediately after dM purification attenuated the increase in M2
126 marker expression on day 7, as illustrated by CD163 and CD206 expression in
127 (Figures 3a and 3b). In addition, no morphological change occurred when IFN-γ was
128 added to the culture medium (Supplementary figure S2b). Seven days of IFN-γ
129 treatment restored IRF5 expression to the level found in freshly purified dM (Figure
130 3c). In parallel, M1 markers (CD64, CD80, CD86) were strongly upregulated by IFN-γ
131 (Figure 3d). However, CD4, CCR5 and DC-SIGN expression on IFN-γ-treated dM
132 varied greatly among donors (Figure 3e). Significantly lower IL-10 and IL-1RA
133 secretion (Figure 3f) and higher chemokine secretion (CCL3, CCL4 and CCL5)
134 (Figure 3g) were detected on day 7 of IFN-γ treatment. Thus, 7 days of IFN-γ
135 treatment restored certain features of freshly purified dM (cell morphology, M2

136 markers and IRF5 expression) and induced certain features of M1 macrophages (M1
137 markers and low IL-10 and IL-1RA secretion).

138 To determine whether IFN-γ treatment affected HIV-1 permissivity, purified dM
139 were challenged with HIV-1/VSV-G on day 7 of culture with and without IFN-γ (Figure
140 4a). IFN-γ impaired HIV-1 replication by more than 80%. This effect was not due to
141 cytotoxicity (Supplementary figure S3a). IFN-γ treatment also impaired dM infection
142 by HIV-1_{BaL}, as shown by p24 Ag quantification in the culture supernatant (Figure
143 4b). By comparison with freshly purified dM, HIV-1 replication was also strongly
144 inhibited in dM (IFN-γ) (Figures 4a and 4c).

145 Together, these results suggest that IFN-γ participates in dM differentiation and
146 contributes to the low permissivity of freshly purified dM to HIV-1 infection.

147

148 **HIV-1 infection of dM (IFN-γ) is inhibited at the reverse-transcription and**
149 **integration steps**

150 As freshly purified dM rapidly switch to an M2 profile and become more
151 susceptible to infection in cytokine-free culture, we used dM (IFN-γ), which recover
152 characteristics of freshly purified dM, to investigate the mechanisms underlying the
153 low permissivity of decidual macrophages.

154 Late reverse transcripts (U5GAG) and integrated proviral DNA that accumulated
155 during the first 48 h of infection by HIV-1/VSV-G in dM (IFN-γ) were quantified and
156 compared to those found in infected dM (US). IFN-γ treatment led to markedly lower
157 levels of U5GAG (Figure 5a) and integrated HIV-1 (Figure 5b). This strongly
158 suggests that HIV-1 infection in dM (IFN-γ) is restricted at early post-entry steps of
159 the replicative cycle.

160

161 **Expression of the cyclin-dependent kinase inhibitor p21Cip1/Waf1 (p21)**
162 **correlates with IRF5 expression and restricts HIV-1 replication in dM (IFN-γ)**

163 We then sought to identify the cellular factor(s) responsible for inhibiting the
164 reverse transcription and integration steps. IFN-γ and IFN-γ-induced factors such as
165 IRF5 are known to modulate the expression of genes involved in cell cycling and
166 apoptosis. We focused on p21, because it has been reported to inhibit HIV-1
167 replication in macrophages [18-20].

168 First, we determined p21 expression by western blot in freshly isolated dM and dM
169 (US) at day 7. Freshly purified dM expressed higher levels of p21 (Figure 6a). Next,
170 we analyzed p21 expression in dM (US) and dM (IFN-γ) at day 7 (Figure 6b). p21
171 was expressed significantly more strongly in dM (IFN-γ) than in dM (US), and
172 correlated with strong IRF5 expression (Figure 6c). p21 expression was then
173 knocked down by short interfering RNA (siRNA) in dM (IFN-γ) prior to challenge with
174 HIV-1/VSV-G (Figure 6d). As a control, we used dM (US) and dM (IFN-γ) treated with
175 random siRNA. p21 silencing in dM (IFN-γ) significantly increased U5GAG levels
176 (Figure 6e) and also the numbers of integrated viral copies (Figure 6f) by comparison
177 with dM (IFN-γ) treated with control siRNA. The resulting levels were not significantly
178 different from those of control dM (US) (Figures 6e and 6f). p21 siRNA had no
179 significant cytotoxic effect, and viability was similar in the three conditions (data not
180 shown). These results show that p21 restricts HIV-1 reverse transcription and
181 integration in dM (IFN-γ).

182 Interestingly, freshly purified dM and dM (IFN-γ) expressed higher levels of p21,
183 than dM (US) (Figure 6a and 6b), suggesting that the increased dM susceptibility to
184 HIV-1 infection in culture is probably associated with a decrease in p21 expression
185 and that IFN-γ addition to the culture medium of freshly purified dM restores both p21

186 expression and low permissivity to infection. Together, these findings suggest that
187 p21 is involved in the control of HIV-1 replication in decidual tissue.
188

189 **TLR7/8 triggering does not alone induce dM polarization towards an M1 or M2**
190 **profile but transiently blocks HIV-1 replication**

191 We have previously shown that dM express functional TLR7/8. We wondered
192 whether these receptors, if activated after HIV-1 sensing, could influence dM
193 polarization and reduce dM susceptibility to infection, as shown for monocytes and
194 MDM [11-14].

195 We first checked whether dM stimulation by a specific agonist (R848) that mimics
196 HIV-1 recognition by TLR7/8 induced a dM polarization switch. dM were treated with
197 R848 immediately after purification or left untreated. TLR7/8 triggering transiently
198 increased CD163 expression on dM after 3 days of R848 treatment, while CD206
199 and M1 expression fell gradually (Figures 7a and 7b). TLR7/8 engagement also
200 down-regulated CD4, CCR5 and DC-SIGN expression (Figure 7c). TLR7/8 triggering
201 by R848 did not induce morphological changes in culture, by comparison to dM (US)
202 (data not shown). Moreover, IRF5 expression was down-regulated in R848-treated
203 dM (Figure 7d). These changes were accompanied by higher IL-10 release by R848-
204 stimulated dM compared to unstimulated dM, whereas IL-1RA secretion was not
205 modified (Figure 7e). Together, these findings show that TLR7/8 activation by itself is
206 not sufficient to fully polarize dM towards an M1 or M2 profile.

207 We then assessed the capacity of R848-stimulated dM to support HIV-1 infection.
208 dM were treated with R848 directly after purification or left untreated, then challenged
209 with HIV-1/VSV-G pseudotyped HIV-1 after 3 days (Figure 8a) or 7 days (Figure 8b)
210 of culture. TLR7/8 triggering impaired HIV-1 replication after 3 days of stimulation,

211 but this antiviral effect had been lost by day 7 (Figure 8c). The inhibitory effect of
212 R848 on HIV-1 replication was not due to cytotoxicity, as viability was unaffected
213 (Supplementary figure S3b). TLR7/8-treated dM were also able to control HIV-1_{BaL}
214 infection, as shown by p24 Ag quantification in the culture supernatant (Figure 8d).
215 We also found that TLR7/8 activation led to accumulation of late RT products (Figure
216 8e) and to a marked decrease in integrated HIV-1 (Figure 8f). These results were
217 consistent with the unmodified p21 expression upon TLR7/8 activation, by
218 comparison to unstimulated dM (data not shown).

219 Together, these results show that TLR7/8 stimulation of dM leads to significant but
220 transient inhibition of HIV-1 replication, after the reverse transcription step and before
221 or at the integration step, potentially reinforcing the low permissivity of dM.

222

223 **TLR7/8 triggering in decidual explants induces M1 polarization of dM and**
224 **restricts HIV-1 replication**

225 We have previously shown that TLR7/8 triggering in dNK cells induces IFN-γ and
226 TNF-α secretion, which could potentially influence dM polarization and HIV-1
227 permissivity [3].

228 Therefore, to determine whether TLR7/8 stimulation can indirectly promote dM
229 polarization, we stimulated cultured decidual explants with R848. Cytokine secretion
230 by R848-treated and untreated explants was measured. Secretion of IFN-γ and of
231 IFN-γ-induced cytokines such as CXCL9 and TNF-α was increased in R848-treated
232 explants (Figure 9a), as was the secretion of both M1 (IL-1β and IL-12) (Figure 9b)
233 and M2 cytokines (IL-1RA and IL-10) (Figure 9c). Secretion of chemokines (CCL3,
234 CCL4 and CCL5) was also increased in R848-treated explants (Figure 9d). To further
235 investigate the effect of TLR7/8 stimulation on dM polarization, decidual explants

236 were digested and the resulting cell suspensions were analyzed by flow cytometry.
237 Untreated and IFN-γ-treated explants were used as negative and positive controls,
238 respectively. TLR7/8 triggering down-regulated the M2 marker CD206 (Figure 9e) as
239 well as HIV-1 receptors and co-receptors (Figure 9f) on the dM surface, and
240 enhanced M1 marker expression (CD64, CD80 and CD86) (Figure 9g). This
241 phenotype modulation was similar to but less marked than that observed with IFN-γ-
242 treated explants.

243 Finally, we checked whether R848-treated explants controlled HIV-1 replication, by
244 adding a TLR7/8 agonist to the explants prior to challenge with HIV-1_{BaL}. HIV-1_{BaL}
245 infection was consistently inhibited in TLR7/8-stimulated explants, as shown by p24
246 Ag measurement (Figure 9h). The viability of R848-treated explants was similar to
247 that of untreated controls (data not shown).

248 TLR7/8 stimulation of decidual explants thus induced dM polarization toward an
249 M1 profile and markedly inhibited HIV-1_{BaL} infection.

250 ## Discussion

251

252 We report for the first time that mucosal macrophages from the *decidua basalis*
253 are characterized by considerable plasticity in their local environment that determine
254 their permissivity to HIV-1 infection.
255 dM have an M2-like phenotype but share features of both M1 (CD64, CD80, CD86
256 and IRF5 expression) and M2 macrophages (CD163 and CD206 expression, IL-1RA
257 and IL-10 secretion). We found that, in culture without exogenous cytokines, dM
258 switched towards a more M2 profile. Thus, dM are likely predestined to adopt an M2
259 program, which is ideally suited to homeostatic remodeling, angiogenesis and
260 tolerogenesis during pregnancy. This is supported here by the observed IL-1RA and
261 IL-10 secretion by dM cultured without exogenous stimuli. IL-10 may play an
262 autocrine/paracrine role in the M2 polarity switch during dM culture [16]. IFN-γ
263 treatment attenuated the increase in M2 marker expression and restored IRF5
264 expression to the level observed in freshly purified dM, suggesting that the presence
265 of IFN-γ in decidual tissue participates in dM differentiation. However, IFN-γ
266 treatment also induced other features of M1 macrophages, such as strong
267 expression of CD64, CD80 and CD86 and weak secretion of IL-10 and IL-1RA. In
268 contrast, it failed to increase IL-12 secretion, in keeping with reports that additional
269 stimuli are needed to induce IL-12 secretion [21,22]. The combined M1 and M2
270 signatures of freshly purified dM are probably ensured by several decidual factors in
271 addition to IFN-γ. In particular, contacts with decidual stromal and mesenchymal cells
272 can induce some M2 features [23]. Phagocytosis of trophoblastic debris generated
273 during pregnancy can also deviate dM toward an M2 phenotype, reducing CD80 and
274 CD86 surface expression and inducing IL-10 and IL-1RA secretion [24]. The balance

275 between these different environmental signals likely accounts for the unique
276 phenotype of freshly purified dM.

277 In parallel to the polarization changes observed in cytokine-free culture, we found
278 that freshly purified dM became more permissive to HIV-1 infection over time. Only
279 CCR5 expression increased significantly over time, possibly playing a role in the
280 increased susceptibility to HIV-1_{BaL} infection, but this would not explain why dM
281 became more sensitive to infection by HIV-1/VSV-G, which does not require the
282 presence of HIV-1 receptors.

283 IFN-γ treatment of dM in culture restored the low permissivity of freshly purified
284 dM, strongly inhibiting the HIV-1 reverse transcription and integration steps. R5 HIV-1
285 entry might also be blocked, as CCR5-binding chemokines (CCL3, CCL4, and CCL5)
286 are strongly induced by IFN-γ [25].

287 Thus, our data demonstrate that dM polarization status is responsible for the low
288 permissivity to HIV-1 infection.

289 As freshly purified dM switch rapidly to an M2 profile in cytokine-free culture, and
290 as IFN-γ prevents this switch (in terms of the phenotype and resistance to infection),
291 we used IFN-γ-treated dM to examine the mechanisms underlying the low
292 permissivity of freshly purified dM, and found that p21 inhibited the reverse
293 transcription and integration steps. This is consistent with a previous study showing
294 that IRF5 modulates the expression of growth-regulating and pro-apoptotic genes,
295 including p21 [18]. However, we cannot exclude the possibility that other IFN-γ-induced
296 genes may modulate p21 expression [20]. We also found that IFN-γ treatment restored
297 p21 expression in culture to a level similar to that of freshly purified dM, suggesting
298 that p21 is involved in HIV-1 restriction in decidual tissue. p21 is known to restrict
299 HIV-1 replication in macrophages either by inhibiting dNTP biosynthesis through a

300 RNR2-dependent pathway [26] or by modulating the phosphorylation of SAMHD1, a
301 host restriction factor [27]. We have previously shown that the SAMHD1 pathway is
302 involved in controlling HIV-1 infection of freshly purified dM [8]. RNR2 was
303 undetectable in dM (IFN-γ), and SAMHD1 phosphorylation was slightly lower in dM
304 (IFN-γ) than in controls, whereas the total SAMHD-1 level remained unchanged
305 (preliminary data not shown). Thus, in decidual tissue, p21 might act through the
306 SAMHD1 pathway.

307 Contrary to IFN-γ, TLR7/8 triggering alone did not induce an M1 or M2 switch.
308 However, TLR7/8 triggering impaired HIV-1/VSV-G infection and resulted in
309 accumulation of late RT products, together with a marked reduction in the amount of
310 integrated proviral DNA. These findings corroborate reports that TLR7/8 ligation
311 impairs HIV-1 infection of monocytes and MDM [12-14,28]. However, as in previous
312 studies [11,29], we found no correlation between the TLR7/8-induced antiviral effect and
313 IFN-α secretion, which was undetectable (data not shown). TLR7/8 engagement
314 down-modulated CD4, CCR5 and DC-SIGN expression and induced secretion of
315 CCR5-binding chemokines [3], which are reported elsewhere to inhibit HIV-1 entry [30].

316 The observed antiviral effects peaked 3 days after TLR7/8 activation and then
317 declined, while the IFN-γ-induced antiviral effect was more profound. This difference
318 was probably due to differential IL-10 secretion by R848- and IFN-γ-treated dM.
319 Indeed, TLR activation induces factors such as IL-10 that restrain TLR-induced
320 inflammatory activation and tissue damage. This inhibitory feedback also seems to
321 control the TLR7/8-induced antiviral effect described above. By contrast, IFN-γ
322 suppresses IL-10 secretion and the IL-10-dependent gene expression that regulate
323 IFN-γ responses. IFN-γ signaling also induces proteins of the IRF family, which in
324 turn generate a second wave of IFN-γ target gene transcription [31].

325 TLR7/8 triggering in purified dM failed to promote an M1 switch. In contrast,
326 TLR7/8 triggering in decidual explants drove dM towards an M1 profile and
327 consistently inhibited HIV-1_{BaL} infection. This M1 switch can be attributed, at least in
328 part, to the increased production of IFN-γ and TNF-α by dNK cells upon TLR7/8
329 activation. Cellular contacts with other decidual cells and other factors induced by
330 TLR7/8 stimulation could also be involved in this switch. Indeed, IL-12 secretion,
331 another hallmark of M1 polarization [4], was also increased in R848-treated explants.
332 This increase could reinforce the dM polarity switch by enhancing dNK secretion of
333 IFN-γ [32]. IL-12-related mechanisms and contacts between dM and dNK cells can also
334 favor the emergence or selection of a macrophage population less sensitive to HIV-1
335 infection [33]. dM switching towards an M1 phenotype could also induce TLR7/8
336 overexpression and thereby further reduce the permissivity of dM to HIV-1 [29]. The
337 durable anti-HIV-1 effect observed in decidual explants is probably due to a
338 synergistic action of TLR7/8 activation and IFN-γ secretion.

339 Mucosal inflammation in the FRT promotes HIV-1 transmission and chronic HIV-1
340 disease [34]. TLR stimulation of other FRT mucosae such as the vaginal mucosa
341 induces proinflammatory cytokine and type I interferon secretion by plasmacytoid
342 dendritic cells (pDC), and enhances viral replication [35]. We found that TLR7/8-
343 stimulated decidual explants increased the secretion of both anti-inflammatory (IL-
344 1RA and IL-10) and pro-inflammatory cytokines (TNF-α and IL-1β). The cytokine
345 profile upon TLR7/8 activation was compatible with the pro/anti-inflammatory
346 cytokine balance required to maintain pregnancy during initiation of an immune
347 response to HIV-1 [3]. This cytokine balance, together with the small number of pDCs
348 and the lack of interferon type I expression in the decidua, may explain these
349 discrepancies.

350 To conclude, our data support a model in which several inter-dependent factors
351 mediate the weak permissivity of dM to HIV-1 infection during the first trimester of
352 pregnancy (Figure 10). In fact, the decidual environment necessary for successful
353 pregnancy is unfavorable to HIV-1 replication. At the maternofetal interface,
354 macrophages acquire distinct phenotypic and functional properties directed by the
355 pro/anti-inflammatory balance (IFN-γ/TNF-α versus IL-10/IL1-RA) and by physical
356 contact with decidual cells. dM therefore have low permissivity to HIV-1 infection.
357 Shortly after infection, p21 blocks HIV-1 reverse transcription and integration. In
358 parallel, TLR7/8, which recognize HIV-1 sequences, are activated and further reduce
359 dM permissivity by adding an extra brake after the reverse transcription step and at
360 or before the integration step. TLR7/8 triggering also induces β-chemokine secretion
361 and down-regulates HIV-1 receptor and co-receptor expression, which may limit viral
362 entry. In addition, TLR7/8 triggering induces IFN-γ and TNF-α release from dNK. This
363 favors an M1 switch of neighboring dM and increases p21 expression, thereby
364 limiting infection of new cells. In parallel, TLR7/8 induce IL-1RA and IL-10 secretion,
365 thereby damping inflammation and preserving the pregnancy (Figure 10).
366 In addition to underlining the role of dM differentiation in HIV-1 control, our findings
367 open new avenues of research into the role of dM differentiation in reproductive
368 immunology and implantation failure.

369 **Materials and Methods**

370

371 **Ethics statement**

372 All the donors in this study provided their written informed consent. The French
373 Biomedicine Agency (n° PF508-013), Assistance Publique des Hôpitaux de Paris (n°
374 VAL/2011/06-41/02) and the Biomedical Research Committee of Institut Pasteur,
375 Paris, France (n° 2005.024) approved the study. The blood used for viral
376 amplification on PBMC were obtained from adult healthy donors (Établissement
377 Français du Sang (n°12/EFS/134 / n° HS2013-24916)). All blood donors signed
378 informed consent allowing the use of their blood for research purpose.

379

380 **Human decidual tissue collection, dM isolation, and reagents**

381 Decidual tissues were obtained from healthy women undergoing voluntary
382 termination of pregnancy during the first trimester (8 - 12 weeks of gestation). dM
383 were purified by positive selection with anti-CD14 magnetic beads. dM purity was
384 checked by flow cytometry and was 93% ± 3.8% (mean + SEM). dM were stimulated
385 3 or 7 days prior to various assays with R848 at 5µg/ml for TLR7/8 activation and
386 IFN-γ at 100ng/ml for dM polarization switch. Detailed procedures are described in
387 the supplementary materials and methods.

388

389 **HIV-1 isolates and infection**

390 For single-round infectious challenge, we used HIV-1 particles (600 ng of p24 Ag/10^6
391 cells) containing the luc reporter gene and pseudotyped with the vesicular stomatitis
392 virus G protein (HIV-1/VSV-G). The efficiency of infection was determined after 72 h
393 by measuring luciferase activity in cell lysates with the Luciferase reagent. For

394 productive infection, HIV-1_{BaL} was used at 10^{-3} MOI. HIV-1_{BaL} replication was
395 measured by p24 Ag ELISA in culture supernatants. Detailed procedures are
396 described in the supplementary materials and methods.
397
398 **Decidual explants**
399 Decidual tissues were cut into 0.3-cm^2 pieces. For flow cytometry, explants were
400 placed on collagen sponge gels in 1.5 ml of medium/well/sponge/piece prior to
401 stimulation with R848 or IFN-γ. Decidual tissue and the sponge were minced,
402 digested and filtered. The total cell population was analyzed by flow cytometry. For
403 experiments with HIV-1_{BaL}, explants were stimulated overnight with R848, then
404 challenged with HIV-1_{BaL} for 12 h. After several washes the explants were placed on
405 collagen sponge gels. All experiments were performed in triplicate. Details are
406 provided in the supplementary materials and methods.
407
408 **Flow cytometry of cell surface markers**
409 Detailed procedures are described in the supplementary materials and methods. In
410 brief, adherent dM were detached from plastic plates by pipetting without scraping.
411 Cells were then incubated with an FcR blocking reagent and stained with conjugated
412 antibodies. Cell surface marker expression was determined with an LSRII 2-Blue 2-
413 Violet 3-Red 5-Yelgr-laser configuration. The results were analyzed with FlowJo
414 9.1.3. software. MFI (%) was calculated as the ratio of treated dM (IFN-γ) or R848-
415 treated dM to the dM (US) control.
416
417 **Western blotting**
418 Details are provided in the supplementary materials and methods. Protein bands

419 intensity were quantified with Image J software 1.47V and normalized to the actin
420 band. The protein band intensity was quantified with the Image J software 1,47V and
421 normalized to the actin band. Ratios (protein / actin) were then compared between
422 the different conditions. Fold changes of IRF5 and p21 expression were calculated by
423 comparing the normalized value of IRF5 and p21 from the IFN-γ-treated samples to
424 the normalized value of IRF5 and p21 from the dM (US) control from the same donor.
425

426 **Cytokine quantification**

427 dM culture supernatants were harvested after 1, 3 or 7 days and stored at -80°C.
428 Soluble factors were measured in a Luminex assay with the Human Cytokine 25-plex
429 antibody bead kit as recommended by the manufacturer (Invitrogen, Saint Aubin,
430 France).
431

432 **siRNA transfection**

433 Small interfering RNAs (siRNAs) were purchased from GE Healthcare Dharmacon
434 (Buckinghamshire, UK). The siRNA against the p21 gene was on-target plus siRNA
435 n.12, and had the following sequence: 5′ AGA CCA GCA UGA CAG AUU U 3′.
436 Control siRNAs (Ctrl) were a pool of four on-target plus nontargeting siRNAs. siRNA
437 transfection was performed using INTERFERin kits (Polyplus Transfection, Illkirch-
438 Graffenstaden, France). 50 nM sip21 or siCtlr was prediluted in 1 mL of Opti-MEM, to
439 which 20 µL of INTERFERin was added. The transfection mix was left at room
440 temperature for 10 min and then incubated with dM at 37°C for 16 hours. Cell culture
441 medium was next replaced by siRNA-free culture medium during 8 hours. The
442 transfection mix was then added for additional 16 hours prior to Western Blot and
443 infection by HIV-1/VSV-G. Ctrl siRNA was also added to dM (US).

444

445 **HIV-1 DNA quantitative PCR (qPCR)**

446 Total DNA in HIV-1/VSV-G-infected dM was extracted 48 h postinfection. Quantitative
447 real-time PCR analysis of late (U5GAG) forms of viral DNA was carried out as
448 previously described [19]. Integrated HIV-1 DNA was quantified by real-time Alu-LTR
449 nested PCR using primers and probes described elsewhere [19]. The amount of viral
450 DNA was normalized to the endogenous reference albumin gene. Detailed
451 procedures are described in supplementary materials and methods.

452

453 **Viability test**

454 The fixable viability dye 329 eFluor 780 (eBiosciences, Paris, France) was used to
455 determine the viability of freshly purified dM and unstimulated dM on day 7 of culture,
456 as recommended by the manufacturer. On days 3 and 7 of culture, the viability of
457 stimulated dM (IFN-γ and R848) and unstimulated dM was also compared. No
458 significant differences were found.

459

460 **Statistical analyses**

461 Statistical analyses were done with GraphPad Prism software version 5.0f. When
462 several groups (>=3) were compared, a Kruskal–Wallis test was used. When this test
463 was significant, two by two comparisons were conducted and a Bonferroni correction
464 was applied. Otherwise the Mann-Whitney test and the Wilcoxon matched pairs test
465 were used. Lines or bars represent the mean, and error bars indicate SEM. The
466 figure legends show in parentheses the number of independent donors used in the
467 experiments. P values <0.05 were considered significant (*$p < 0.05$, **$p < 0.005$, ***p
468 < 0.0005, ****$p < 0.0001$). (#) Represents the statistical comparison of MFI values

469 between stimulated and unstimulated dM at a given time point. ($^{\#}p < 0.05$, $^{\#\#}p <$
470 0.005, $^{\#\#\#}p < 0.0005$, $^{\#\#\#\#}p < 0.0001$).
471
472 **DISCLOSURES**
473 The authors declared no conflict of interest.
474

475 Acknowledgments

476 The authors thank Dr G Chaouat, A Saez-Cirion, G Pancino, J C Valle Casuso and P
477 Lebouteiller for scientific discussions, D. Young for critical editing of the manuscript
478 and Dr Y Madec for his advice for statistical analysis. We also thank all the women
479 who gave their informed consent, AP-HP (Assistance Publique Hôpitaux de Paris),
480 Anne Lebreton, Séverine Ballan and clinical personnel for providing the samples;
481 PIRC (Pole Intégré de Recherche Clinique, Institut Pasteur) for help with regulatory
482 aspects; and Centre d'Immunologie Humaine, Institut Pasteur, for Luminex assay.
483 This work was supported by ANRS (H.E-C and H.Q financial support and grant
484 #12165/13129), Sidaction (H.E-C and M.D financial support and grant # AI20-3-
485 01671), the TOTAL Foundation, INSERM, and Institut Pasteur.

References

1 Chouquet, C., Burgard, M., Richardson, S., Rouzioux, C. & Costagliola, D. Timing of mother-to-child HIV-1 transmission and diagnosis of infection based on polymerase chain reaction in the neonatal period by a non-parametric method. Aids 11, 1183-1184 (1997).

2 Marlin, R. et al. Antigen-presenting cells represent targets for R5 HIV-1 infection in the first trimester pregnancy uterine mucosa. PLoS One 4, e5971, doi:10.1371/journal.pone.0005971 (2009).

3 Duriez, M. et al. Human decidual macrophages and NK cells differentially express Toll-like receptors and display distinct cytokine profiles upon TLR stimulation. Front Microbiol 5, 316, doi:10.3389/fmicb.2014.00316 (2014).

4 Krausgruber, T. et al. IRF5 promotes inflammatory macrophage polarization and TH1-TH17 responses. Nat Immunol 12, 231-238, doi:10.1038/ni.1990 (2011).

5 Biswas, S. K. & Mantovani, A. Macrophage plasticity and interaction with lymphocyte subsets: cancer as a paradigm. Nat Immunol 11, 889-896, doi:10.1038/ni.1937 (2010).

6 Martinez, F. O. & Gordon, S. The M1 and M2 paradigm of macrophage activation: time for reassessment. F1000Prime Rep 6, 13, doi:10.12703/P6-13 (2014).

7 Cassetta, L. et al. M1 polarization of human monocyte-derived macrophages restricts pre and postintegration steps of HIV-1 replication. Aids 27, 1847-1856, doi:10.1097/QAD.0b013e328361d059 (2013).

8 Quillay, H. et al. Distinct Characteristics of Endometrial and Decidual Macrophages and Regulation of Their Permissivity to HIV-1 Infection by SAMHD1. J Virol 89, 1329-1339, doi:10.1128/JVI.01730-14 (2015).

9 Siewiera, J. et al. Human cytomegalovirus infection elicits new decidual natural killer cell effector functions. PLoS Pathog 9, e1003257, doi:10.1371/journal.ppat.1003257 (2013).

10 Heil, F. et al. Species-specific recognition of single-stranded RNA via toll-like receptor 7 and 8. Science 303, 1526-1529, doi:10.1126/science.1093620 (2004).

11 Wang, X., Chao, W., Saini, M. & Potash, M. J. A common path to innate immunity to HIV-1 induced by Toll-like receptor ligands in primary human macrophages. PLoS One 6, e24193, doi:10.1371/journal.pone.0024193 (2011).

12 Campbell, G. R. & Spector, S. A. Toll-like receptor 8 ligands activate a vitamin D mediated autophagic response that inhibits human immunodeficiency virus type 1. PLoS Pathog 8, e1003017, doi:10.1371/journal.ppat.1003017 (2012).

13 Nian, H. et al. R-848 triggers the expression of TLR7/8 and suppresses HIV replication in monocytes. BMC Infect Dis 12, 5, doi:10.1186/1471-2334-12-5 (2012).

14 Sica, A. & Mantovani, A. Macrophage plasticity and polarization: in vivo veritas. J Clin Invest 122, 787-795, doi:10.1172/JCI59643 (2012).

15 Seledtsov, V. I. & Seledtsova, G. V. A balance between tissue-destructive and tissue-protective immunities: a role of toll-like receptors in regulation of

533 adaptive immunity. Immunobiology 217, 430-435,
534 doi:10.1016/j.imbio.2011.10.011 (2012).
535 16 Mantovani, A., Biswas, S. K., Galdiero, M. R., Sica, A. & Locati, M.
536 Macrophage plasticity and polarization in tissue repair and remodelling. J
537 Pathol 229, 176-185, doi:10.1002/path.4133 (2013).
538 17 Schoenborn, J. R. & Wilson, C. B. Regulation of interferon-gamma during
539 innate and adaptive immune responses. Adv Immunol 96, 41-101,
540 doi:10.1016/S0065-2776(07)96002-2 (2007).
541 18 Barnes, B. J., Kellum, M. J., Pinder, K. E., Frisancho, J. A. & Pitha, P. M.
542 Interferon regulatory factor 5, a novel mediator of cell cycle arrest and cell
543 death. Cancer Res 63, 6424-6431 (2003).
544 19 Bergamaschi, A. et al. The CDK inhibitor p21Cip1/WAF1 is induced by
545 FcgammaR activation and restricts the replication of human immunodeficiency
546 virus type 1 and related primate lentiviruses in human macrophages. J Virol
547 83, 12253-12265, doi:10.1128/JVI.01395-09 (2009).
548 20 Armstrong, M. J. et al. Interferon Regulatory Factor 1 (IRF-1) induces
549 p21(WAF1/CIP1) dependent cell cycle arrest and p21(WAF1/CIP1)
550 independent modulation of survivin in cancer cells. Cancer Lett 319, 56-65,
551 doi:10.1016/j.canlet.2011.12.027 (2012).
552 21 Skeen, M. J., Miller, M. A., Shinnick, T. M. & Ziegler, H. K. Regulation of
553 murine macrophage IL-12 production. Activation of macrophages in vivo,
554 restimulation in vitro, and modulation by other cytokines. J Immunol 156,
555 1196-1206 (1996).
556 22 Lombardelli, L. et al. HLA-G5 induces IL-4 secretion critical for successful
557 pregnancy through differential expression of ILT2 receptor on decidual CD4(+)
558 T cells and macrophages. J Immunol 191, 3651-3662,
559 doi:10.4049/jimmunol.1300567 (2013).
560 23 Kim, J. & Hematti, P. Mesenchymal stem cell-educated macrophages: a novel
561 type of alternatively activated macrophages. Exp Hematol 37, 1445-1453,
562 doi:10.1016/j.exphem.2009.09.004 (2009).
563 24 Abumaree, M. H., Chamley, L. W., Badri, M. & El-Muzaini, M. F. Trophoblast
564 debris modulates the expression of immune proteins in macrophages: a key to
565 maternal tolerance of the fetal allograft? J Reprod Immunol 94, 131-141,
566 doi:10.1016/j.jri.2012.03.488 (2012).
567 25 Marlin, R. et al. Decidual soluble factors participate in the control of HIV-1
568 infection at the maternofetal interface. Retrovirology 8, 58, doi:10.1186/1742-
569 4690-8-58 (2011).
570 26 Allouch, A. et al. p21-mediated RNR2 repression restricts HIV-1 replication in
571 macrophages by inhibiting dNTP biosynthesis pathway. Proc Natl Acad Sci U
572 S A 110, E3997-4006, doi:10.1073/pnas.1306719110 (2013).
573 27 Allouch, A. et al. Reply to Pauls et al.: p21 is a master regulator of HIV
574 replication in macrophages through dNTP synthesis block. Proc Natl Acad Sci
575 U S A 111, E1325-1326 (2014).
576 28 Buitendijk, M., Eszterhas, S. K. & Howell, A. L. Toll-like receptor agonists are
577 potent inhibitors of human immunodeficiency virus-type 1 replication in
578 peripheral blood mononuclear cells. AIDS Res Hum Retroviruses 30, 457-467,
579 doi:10.1089/AID.2013.0199 (2014).
580 29 Schlaepfer, E., Rochat, M. A., Duo, L. & Speck, R. F. Triggering TLR2, -3, -4, -
581 5, and -8 reinforces the restrictive nature of M1- and M2-polarized
582 macrophages to HIV. J Virol 88, 9769-9781, doi:10.1128/JVI.01053-14 (2014).

30 Lehner, T. et al. Up-regulation of beta-chemokines and down-modulation of CCR5 co-receptors inhibit simian immunodeficiency virus transmission in non-human primates. Immunology 99, 569-577 (2000).

31 Hu, X., Chakravarty, S. D. & Ivashkiv, L. B. Regulation of interferon and Toll-like receptor signaling during macrophage activation by opposing feedforward and feedback inhibition mechanisms. Immunol Rev 226, 41-56, doi:10.1111/j.1600-065X.2008.00707.x (2008).

32 O'Donnell, M. A. et al. Role of IL-12 in the induction and potentiation of IFN-gamma in response to bacillus Calmette-Guerin. J Immunol 163, 4246-4252 (1999).

33 Bellora, F. et al. The interaction of human natural killer cells with either unpolarized or polarized macrophages results in different functional outcomes. Proc Natl Acad Sci U S A 107, 21659-21664, doi:10.1073/pnas.1007654108 (2010).

34 Joseph, T. et al. Induction of cyclooxygenase (COX)-2 in human vaginal epithelial cells in response to TLR ligands and TNF-alpha. Am J Reprod Immunol 67, 482-490, doi:10.1111/j.1600-0897.2011.01099.x (2012).

35 Wang, Y. et al. The Toll-like receptor 7 (TLR7) agonist, imiquimod, and the TLR9 agonist, CpG ODN, induce antiviral cytokines and chemokines but do not prevent vaginal transmission of simian immunodeficiency virus when applied intravaginally to rhesus macaques. J Virol 79, 14355-14370, doi:10.1128/JVI.79.22.14355-14370.2005 (2005).

606 ## Figure legends

607

608 **Figure 1. dM become more permissive to HIV-1 infection in cytokine-free**
609 **culture.**

610 (a) Freshly purified dM were challenged with HIV-1/VSV-G at day 0, 3 and 7 of
611 culture. HIV-1 replication was monitored by measuring luciferase activity (n=7).

612 (b) dM were challenged with HIV-1_{BaL} immediately after isolation (day 0) or after 7
613 days of cytokine-free culture. Viral production was followed by quantifying p24 Ag in
614 the supernatant. p24 Ag production on day 21 post-infection (n=7).

615 Mean ± SEM of *n* independent donors.

616

617 **Figure 2. dM switch towards a more M2 profile in cytokine-free culture.**

618 (a) Representative histograms of CD163 and CD206 expression on dM, as measured
619 by flow cytometry.

620 (b) CD163 and CD206 mean fluorescent intensity (MFI) over time (n=6).

621 (c) CD4, CCR5 and DC-SIGN mean fluorescent intensity (MFI) on day 0 and on day
622 7 of culture (n=6).

623 (d) Representative western blot of IRF5 expression by dM over time (left panel). The
624 protein band intensity was quantified and normalized to the actin band. Ratio (IRF5 /
625 actin) was then compared over time (right panel) (n=6).

626 (e) dM cytokine release after 1, 3 and 7 days of culture (n=6).

627 Mean ± SEM of *n* independent donors.

628

629

630

631 **Figure 3. IFN-γ addition to cultured dM restores partially the phenotype of**
632 **freshly purified dM.**
633 (a) Representative histograms of IFN-γ-induced modulation of CD163 and CD206
634 expression on day 7, as measured by flow cytometry.
635 (b) IFN-γ-induced change (%) in CD163 and CD206 expression (MFI) on dM
636 compared to time-matched unstimulated dM (n=6).
637 (c) Representative western blot of IRF5 expression by IFN-γ-stimulated and
638 unstimulated dM on day 7 of culture (left panel). The protein band intensity was
639 quantified and normalized to the actin band. Ratio (IRF5 / actin) was then compared
640 between IFN-γ-stimulated and unstimulated dM on day 7 of culture (right panel)
641 (n=19).
642 (d) IFN-γ-induced change (%) in CD64, CD80 and CD86 expression (MFI) on dM, as
643 compared to time-matched unstimulated dM (n=6).
644 (e) IFN-γ-induced changes (%) in CD4, DC-SIGN and CCR5 expression (MFI) on dM
645 on day 7 of culture, by comparison with unstimulated dM (n=17).
646 (f) dM cytokine and (G) β-chemokine release after 7 days of culture (n=7).
647 Mean ± SEM of *n* independent donors. # = statistical comparison of MFI values
648 between IFN-γ-stimulated dM versus unstimulated (US) dM at the same time.
649
650 **Figure 4. IFN-γ addition to cultured dM restores the resistance to HIV-1.**
651 (a) Freshly purified dM and 7-day IFN-γ-stimulated and unstimulated (US) dM were
652 challenged with HIV-1/VSV-G. HIV-1 replication was monitored by measuring
653 luciferase activity in cell lysates (n=13).
654 (b) IFN-γ stimulated and US dM were challenged with HIV-1_{BaL} on day 7 of culture.
655 HIV-1 p24 Ag was measured by ELISA in the supernatants (n=6).

656 (c) p24 Ag production on day 21 after infection by HIV-1_{BaL} was compared between
657 freshly purified dM and 7-day IFN-γ-stimulated or unstimulated dM (n=6).
658 Mean ± SEM of *n* independent donors.
659
660
661 **Figure 5. IFN-γ restricts HIV-1 infection of dM at the reverse transcription and**
662 **integration steps.**
663 7-day IFN-γ-stimulated and unstimulated (US) dM were challenged with HIV-1/VSV-
664 G. Late reverse-transcription products (U5GAG) (n=6) (a) and integrated forms (n=8)
665 (b) were quantified by qPCR. Mean ± SEM of *n* independent donors.
666
667 **Figure 6. p21 is involved in low dM permissivity to HIV-1.**
668 (a) Representative western blot of p21 expression by freshly purified dM (day 0) and
669 by unstimulated dM at day 7 of culture (left panel). The protein band intensity was
670 quantified and normalized to the actin band. Ratio (p21 / actin) was then compared
671 between dM at day 0 and day 7 (right panel) (n=6).
672 (b) Representative western blot of p21 expression by IFN-γ-stimulated and
673 unstimulated (US) dM on day 7 of culture (left panel). Ratio (p21 / actin) was then
674 compared between the 7-days IFN-γ-stimulated and unstimulated (US) (right panel)
675 (n=20).
676 (c) Fold changes of IRF5 and p21 expression were calculated by comparing the
677 normalized value of IRF5 and p21 from the IFN-γ-treated samples to the normalized
678 value of IRF5 and p21 from the dM (US) control.
679 Correlation between fold changes in IRF5 and p21 expression on day 7 of IFN-γ
680 treatment compared to time-matched unstimulated dM (n=19). Spearman's R value is

681 shown.

682 (d) Representative western blot of p21 expression in 7-day IFN-γ-stimulated and
683 unstimulated dM transfected with p21-specific siRNA or with an irrelevant control
684 siRNA (Ctrl) (n=9).

685 (e) Number of late reverse transcription products (U5GAG) and (F) integrated forms
686 in dM transfected with p21-specific or control siRNA (n=9).

687 Mean ± SEM of *n* independent donors.

688

689 **Figure 7. TLR7/8 triggering is not sufficient to induce dM polarization towards**
690 **an M1 or M2 profile.**

691 (a) % change in dM CD163 and CD206, (b) CD64, CD80 and CD86 expression (MFI)
692 induced by R848 as compared to time-matched unstimulated dM.

693 (c) % change in dM CD4, DC-SIGN and CCR5 expression (MFI) induced by R848 as
694 compared to time-matched unstimulated dM.

695 (d) Ratio of IRF5 to actin expression by R848-stimulated and unstimulated dM on
696 days 3 and 7 of culture.

697 (e) dM cytokine release after 3 days of culture.

698 Mean ± SEM of 6 independent donors. # = statistical comparison of MFI values
699 between R848-stimulated versus unstimulated dM at the same time.

700

701 **Figure 8. TLR7/8 triggering restricts HIV-1 replication after the reverse**
702 **transcription step and at or before the integration step.**

703 R848-stimulated and unstimulated (US) dM were challenged with HIV-1/VSV-G on
704 day 3 (n=13) (a) or day 7 (n=6) (b) of culture. HIV-1 replication was monitored by
705 measuring luciferase activity. The % of luciferase activity inhibition was determined

706 by comparison with time-matched unstimulated dM (c).

707 (d) R848-stimulated and US dM were challenged with HIV-1_{BaL} on day 3 of culture.
708 HIV-1 p24 Ag was measured by ELISA in the culture supernatants (n=9)

709 Late reverse transcription products (U5GAG) (n=8) (e) and integrated forms (n=8) (f)
710 were quantified by qPCR in dM infected with HIV-1/VSV-G on day 3. Mean ± SEM of
711 *n* independent donors.

712

713

714 **Figure 9. TLR7/8 triggering in decidual explants induces M1 polarization of dM**
715 **and restricts HIV-1 replication**

716 Decidual explants were stimulated with R848 or left unstimulated (US).

717 (a) (b) (c) (d) cytokine and β-chemokine concentrations in explant supernatants after
718 3 days of culture.

719 (e) (f) (g) Marker expression on $CD45^+$ $CD14^+$ dM after explant digestion on day 7 of
720 culture, as measured by flow cytometry of total decidual cells. The % change in MFI
721 induced by R848 and IFN-γ was determined by comparison with time-matched
722 unstimulated explants.

723 (h) Explants were stimulated with R848 or left untreated prior to challenge with HIV-
724 1_{BaL}. HIV-1 p24 Ag was measured by ELISA in explant supernatants.

725 Mean ± SEM of 7 independent donors. # = statistical comparison of MFI values
726 between R848-stimulated versus unstimulated dM.

727

728 **Figure 10. Integrated model of the inter-dependent factors involved in dM**
729 **differentiation and natural resistance to HIV-1 infection.**

730 In case of HIV-1 infection, p21 blocks HIV-1 replication at the reverse transcription

731 and integration steps (1). In parallel, TLR7/8 activation by HIV-1 sequences (2), add
732 an extra brake after the reverse transcription step and at or before the integration
733 step (3). TLR7/8 triggering may also limit viral entry by inducing β-chemokine
734 secretion (4) and by down-regulating HIV-1 receptor and co-receptor expression (5).
735 In addition, TLR7/8 triggering induces IFN-γ and TNF-α release from dNK cells (6),
736 which favors an M1 switch of neighboring dM (7) and increases p21 expression (8).
737 In parallel, TLR7/8 induce IL-1RA and IL-10 secretion that restrain TLR-induced
738 inflammatory activation and tissue damage (9). In conclusion, the decidual pro/anti-
739 inflammatory cytokine balance shape the phenotype of dM and their permissivity to
740 HIV-1 infection (10).

Figure 1

a

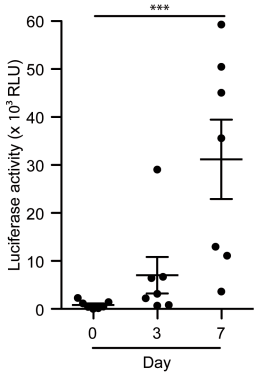
***
Luciferase activity (x 10³ RLU)
60
50
40
30
20
10
0
0
3
7
Day

b

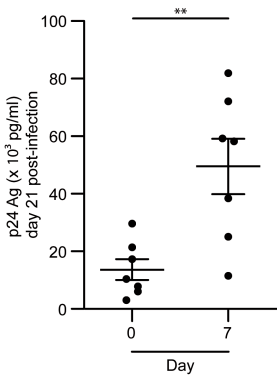
**
p24 Ag (x 10³ pg/ml)
day 21 post-infection
100
80
60
40
20
0
0
7
Day

Figure 2

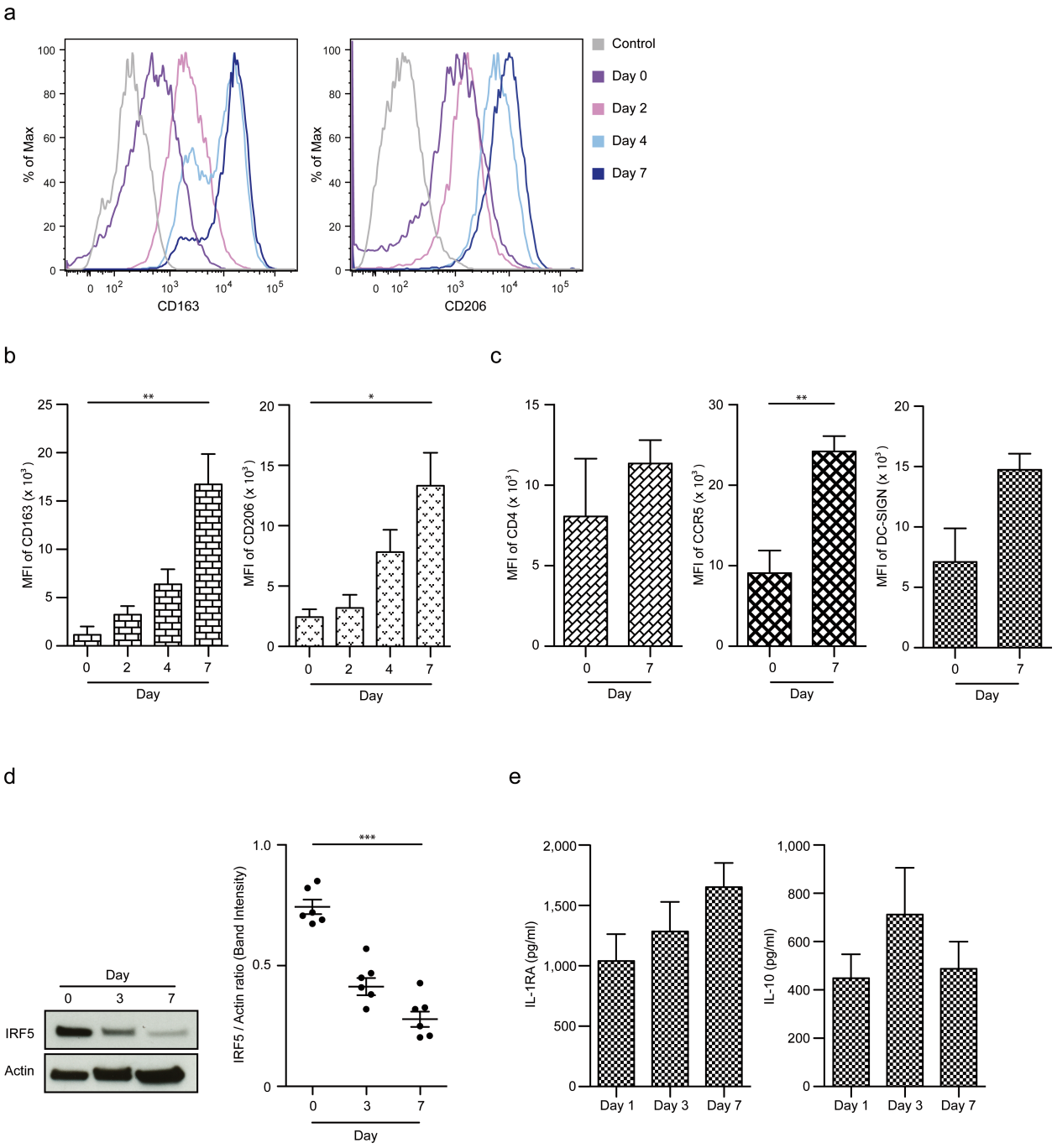
a
% of Max
CD163
CD206
Control
Day 0
Day 2
Day 4
Day 7
b
MFI of CD163 (x 10³)
MFI of CD206 (x 10³)
Day
c
MFI of CD4 (x 10³)
MFI of CCR5 (x 10³)
MFI of DC-SIGN (x 10³)
d
Day
IRF5
Actin
IRF5 / Actin ratio (Band Intensity)
e
IL-1RA (pg/ml)
IL-10 (pg/ml)
Day 1
Day 3
Day 7

Figure 3

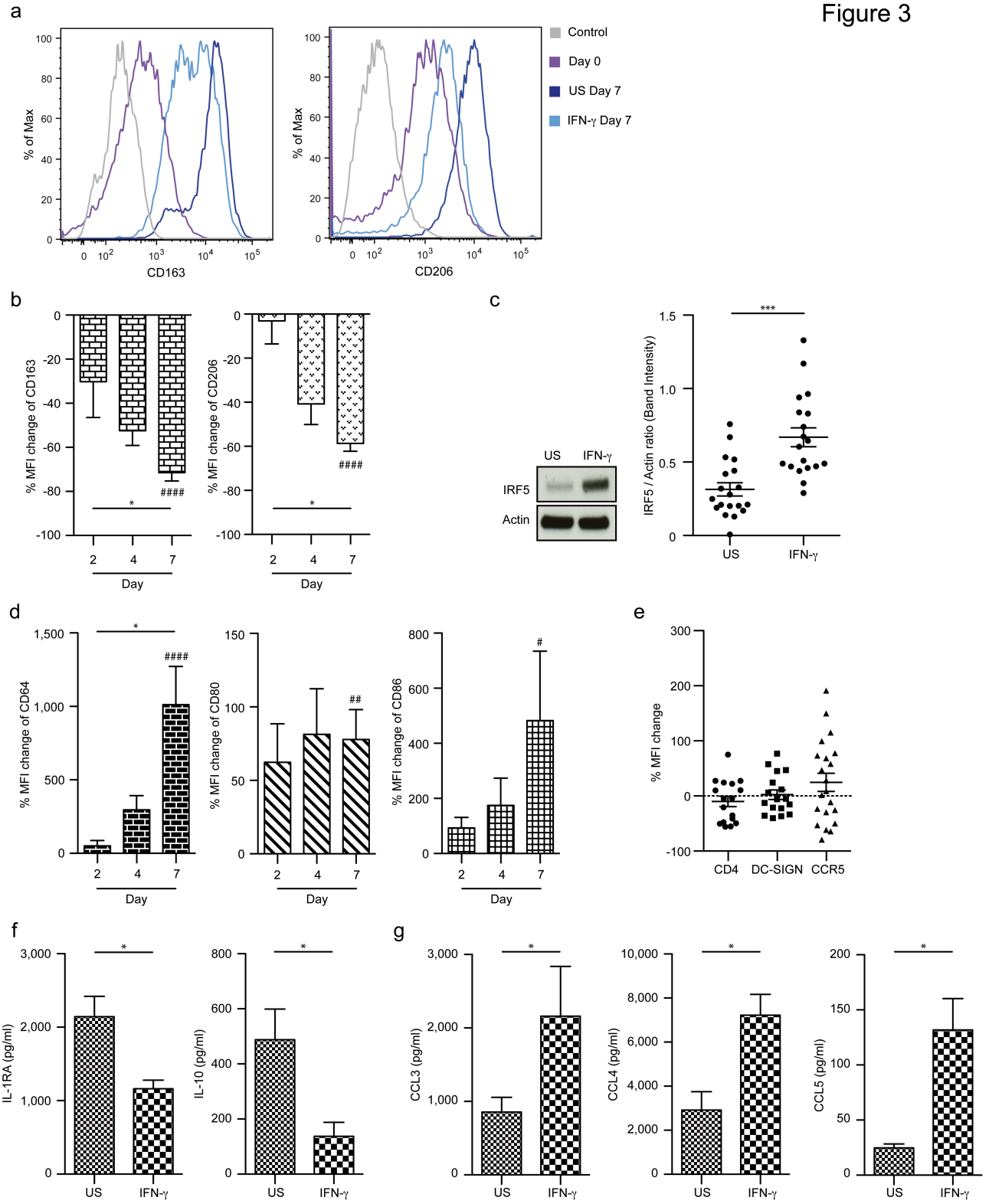
a
% of Max
CD163
CD206
Control
Day 0
US Day 7
IFN-γ Day 7
b
% MFI change of CD163
% MFI change of CD206
Day
c
US
IFN-γ
IRF5
Actin
IRF5 / Actin ratio (Band Intensity)
d
% MFI change of CD64
% MFI change of CD80
% MFI change of CD86
e
% MFI change
CD4
DC-SIGN
CCR5
f
IL-1RA (pg/ml)
IL-10 (pg/ml)
g
CCL3 (pg/ml)
CCL4 (pg/ml)
CCL5 (pg/ml)

Figure 4

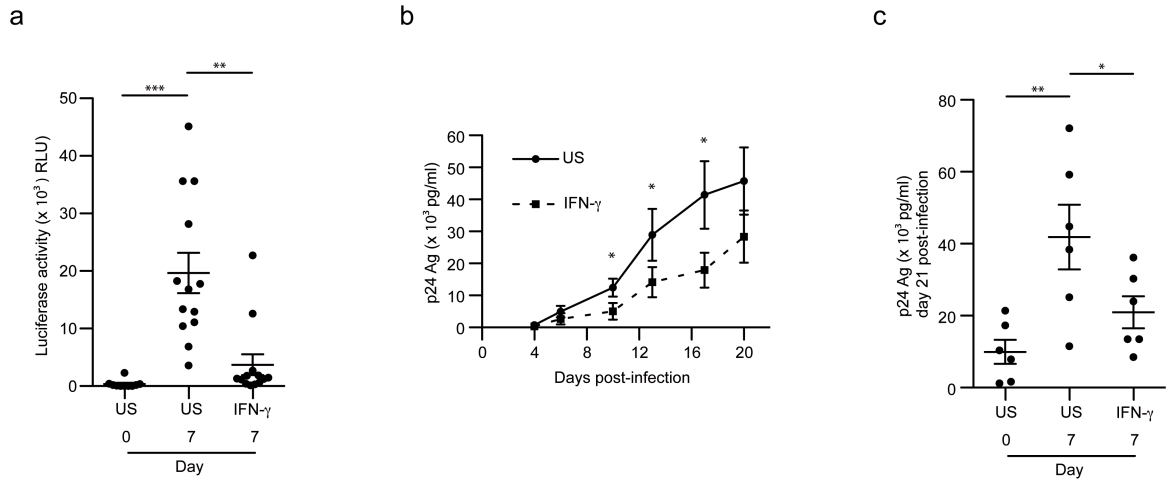
a
b
c
Luciferase activity (x 10³) RLU)
***
**
US
US
IFN-γ
0
7
7
Day
p24 Ag (x 10³ pg/ml)
US
IFN-γ
Days post-infection
p24 Ag (x 10³ pg/ml)
day 21 post-infection

Figure 5

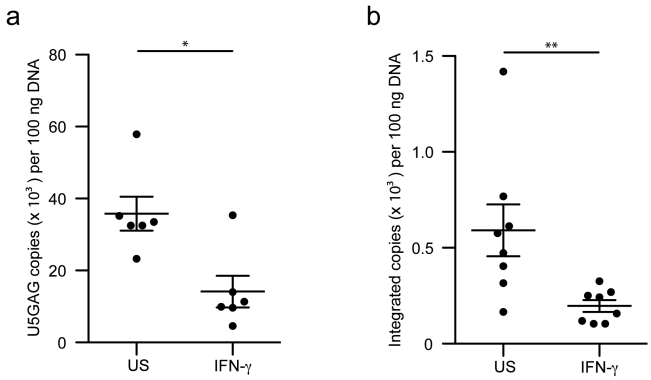
a
*
80
60
40
20
0
U5GAG copies (x 10³) per 100 ng DNA
US
IFN-γ
b
**
1.5
1.0
0.5
0
Integrated copies (x 10³) per 100 ng DNA
US
IFN-γ

Figure 6

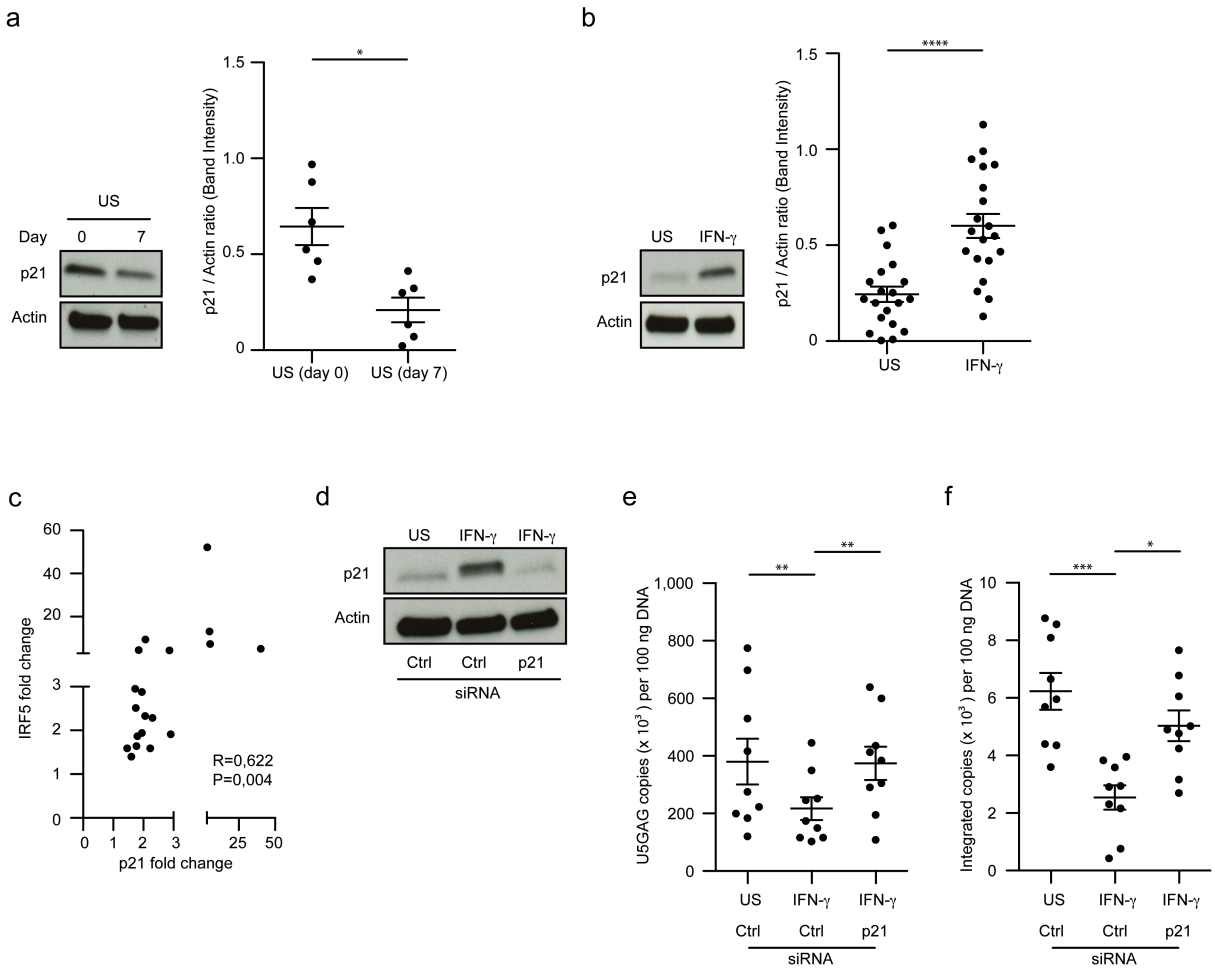
a
US
Day 0 7
p21
Actin
p21 / Actin ratio (Band Intensity)
1.5
1.0
0.5
0
*
US (day 0)
US (day 7)
b
US IFN-γ
p21
Actin
p21 / Actin ratio (Band Intensity)
****
US
IFN-γ
c
IRF5 fold change
60
40
20
3
2
1
0
R=0,622
P=0,004
0 1 2 3 25 50
p21 fold change
d
US IFN-γ IFN-γ
p21
Actin
Ctrl Ctrl p21
siRNA
e
U5GAG copies (x 10³) per 100 ng DNA
1,000
800
600
400
200
0
**
**
US IFN-γ IFN-γ
Ctrl Ctrl p21
siRNA
f
Integrated copies (x 10³) per 100 ng DNA
10
8
6
4
2
0
***
*
US IFN-γ IFN-γ
Ctrl Ctrl p21
siRNA

Figure 7

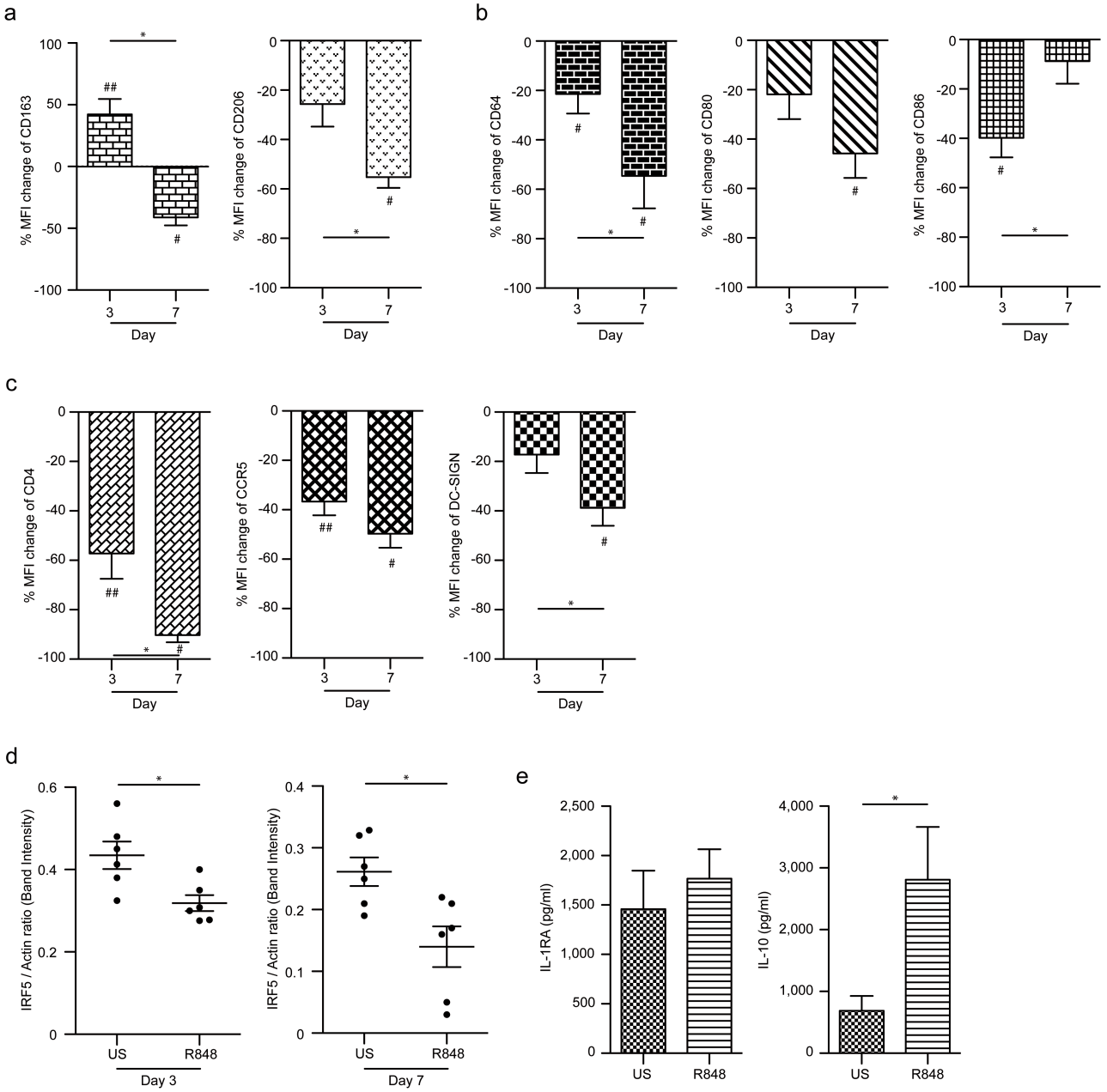
a
% MFI change of CD163
% MFI change of CD206
b
% MFI change of CD64
% MFI change of CD80
% MFI change of CD86
Day
c
% MFI change of CD4
% MFI change of CCR5
% MFI change of DC-SIGN
d
IRF5 / Actin ratio (Band Intensity)
US
R848
Day 3
Day 7
e
IL-1RA (pg/ml)
IL-10 (pg/ml)

Figure 8

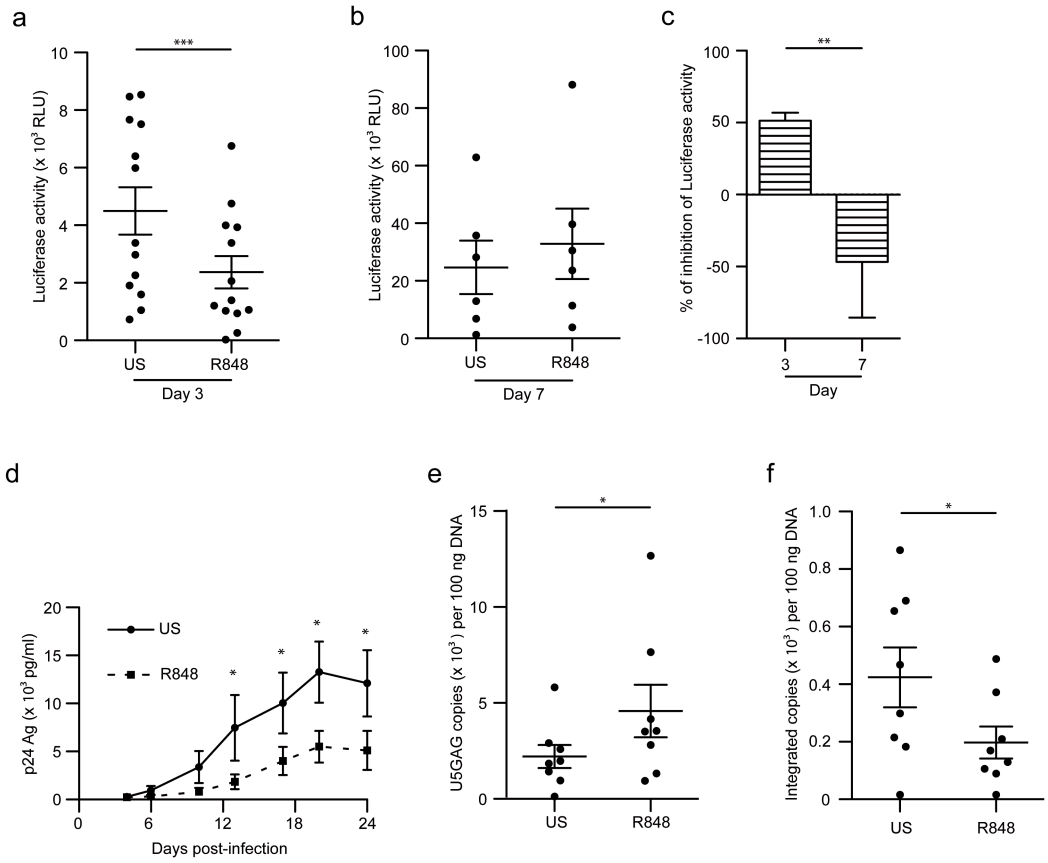
a
***
Luciferase activity (x 10³ RLU)
10
8
6
4
2
0
US
R848
Day 3
b
Luciferase activity (x 10³ RLU)
100
80
60
40
20
0
US
R848
Day 7
c
**
% of inhibition of Luciferase activity
100
50
0
-50
-100
3
7
Day
d
p24 Ag (x 10³ pg/ml)
20
15
10
5
0
US
R848
*
0
6
12
18
24
Days post-infection
e
*
U5GAG copies (x 10³) per 100 ng DNA
15
10
5
0
US
R848
f
*
Integrated copies (x 10³) per 100 ng DNA
1.0
0.8
0.6
0.4
0.2
0
US
R848

Figure 9

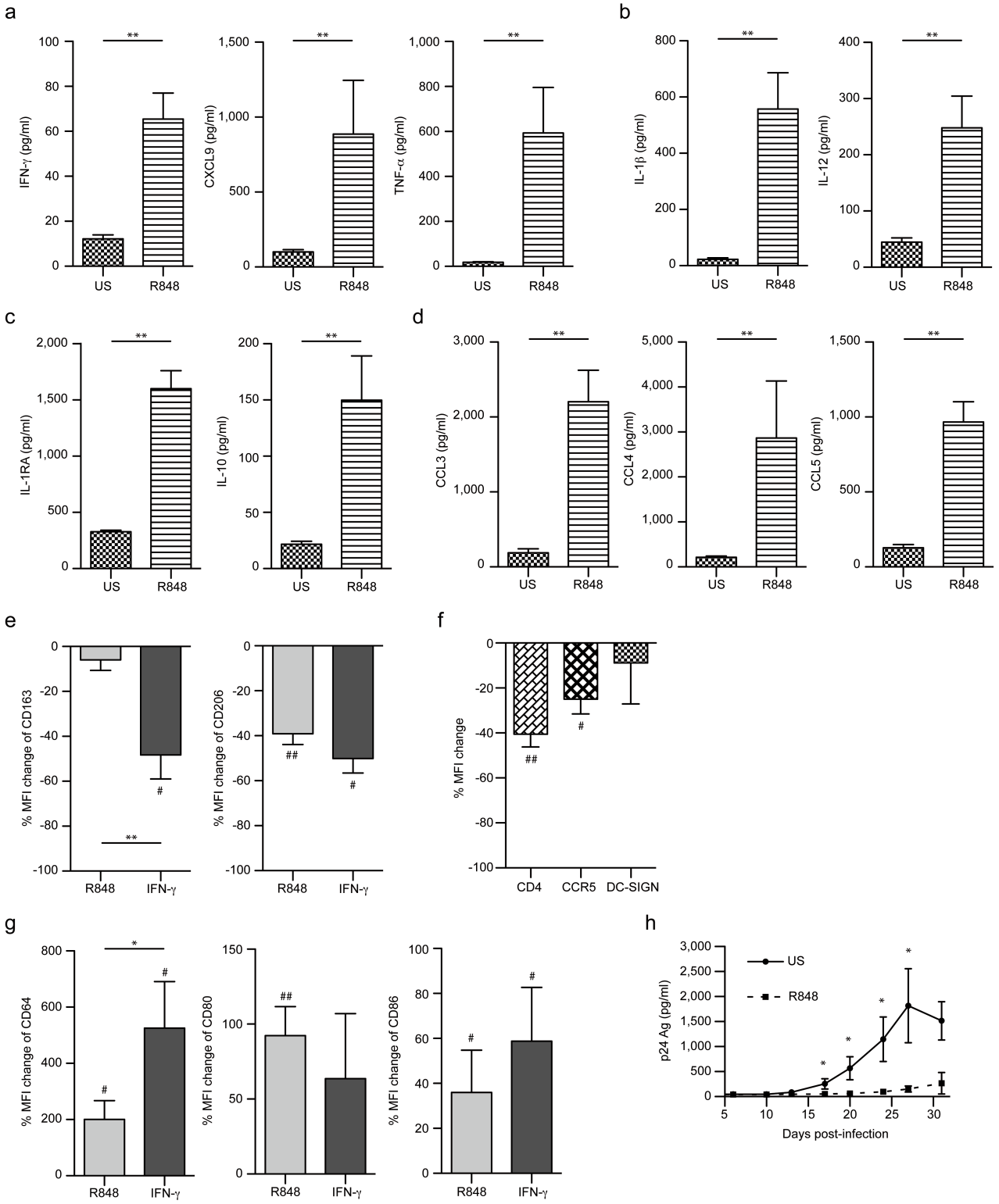
a
IFN-γ (pg/ml)
CXCL9 (pg/ml)
TNF-α (pg/ml)
b
IL-1β (pg/ml)
IL-12 (pg/ml)
c
IL-1RA (pg/ml)
IL-10 (pg/ml)
d
CCL3 (pg/ml)
CCL4 (pg/ml)
CCL5 (pg/ml)
US
R848
e
% MFI change of CD163
% MFI change of CD206
R848
IFN-γ
f
% MFI change
CD4
CCR5
DC-SIGN
g
% MFI change of CD64
% MFI change of CD80
% MFI change of CD86
R848
IFN-γ
h
p24 Ag (pg/ml)
US
R848
Days post-infection

Figure 10

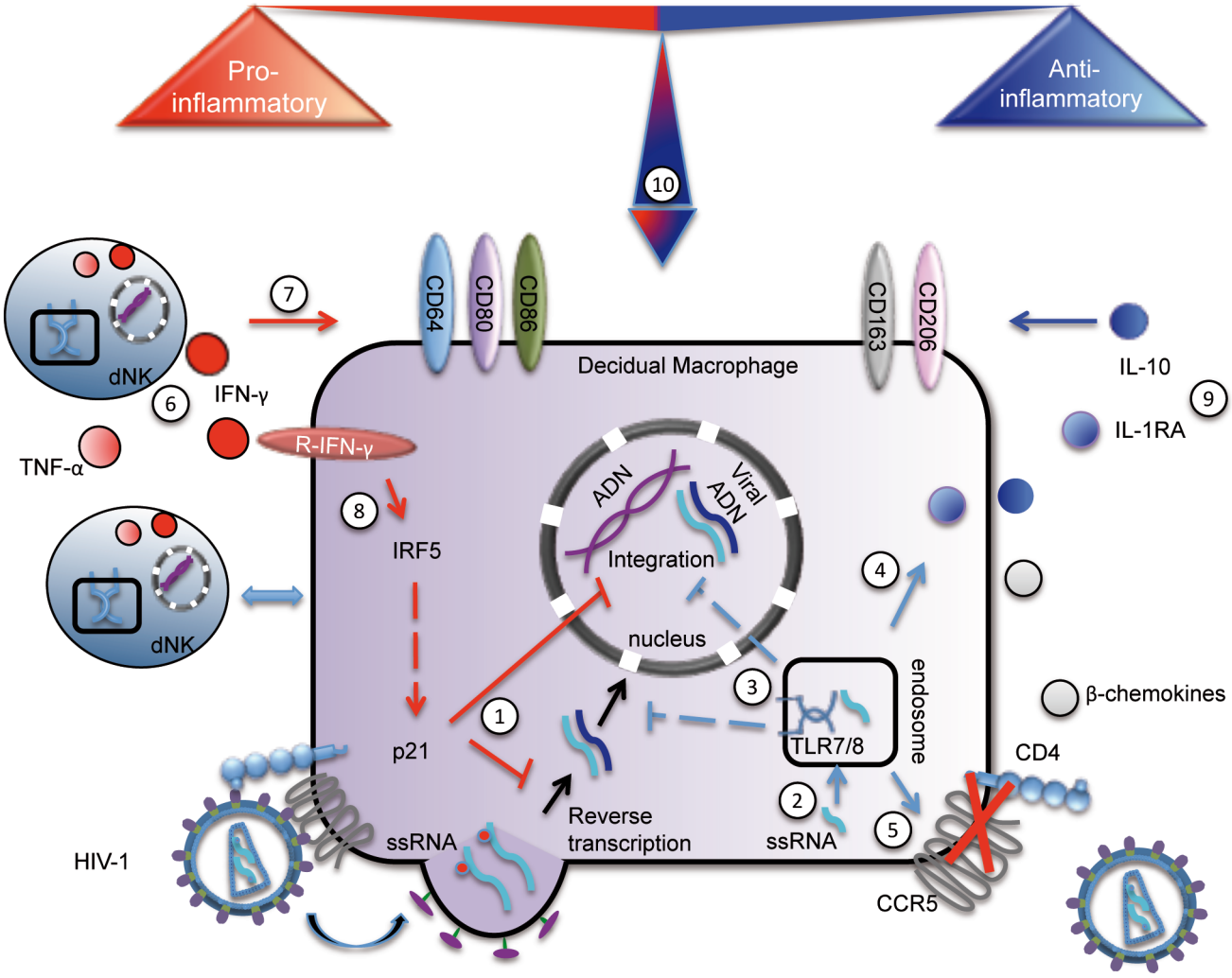
Pro-
inflammatory
Anti-
inflammatory
10
7
CD64
CD80
CD86
CD163
CD206
Decidual Macrophage
IL-10
9
IL-1RA
dNK
6
IFN-γ
TNF-α
R-IFN-γ
8
IRF5
ADN
Viral
ADN
Integration
nucleus
4
dNK
3
endosome
β-chemokines
1
p21
TLR7/8
CD4
2
Reverse
transcription
ssRNA
ssRNA
5
HIV-1
CCR5

Supplementary figure legends

Supplementary Figure S1. M1 marker expression on dM in cytokine-free culture.

(a) (b) (c) CD64, CD80 and CD86 mean fluorescent intensity (MFI) over time. Mean ± SEM of 6 independent donors.

Supplementary Figure S2. dM morphology in culture.

Morphology of unstimulated (US) (a) and IFN-γ-stimulated (b) dM on days 2 and 7 of culture.

Bars = 100 µm. Original magnification X40.

Supplementary Figure S3. Viability of IFN-γ- and R848-stimulated dM.

(a) Viability of IFN-γ–stimulated and unstimulated (US) dM after 7 days of culture, as measured by flow cytometry after labeling dead cells. A representative FACS dot plot gated on $CD45^+$ $CD14^+$ dM is shown.

(b) Viability of R848-stimulated and US dM after 3 days of culture, as measured by flow cytometry. A representative FACS dot plot gated on $CD45^+$ $CD14^+$ dM is shown.

Supplementary Materials and Methods

Human decidual tissue collection, dM isolation, and reagents

Decidual tissues were obtained from healthy women undergoing voluntary termination of pregnancy during the first trimester (8 - 12 weeks of gestation) at Antoine Béclère Hospital (Clamart, France) or Pitié-Salpêtrière Hospital (Paris,

France). After isolation, the decidua was minced and digested with 1 mg/mL collagenase IV (Sigma, St Quentin Fallavier, France) and 250 U/mL recombinant DNase I (Roche, Meylan, France) for 45 minutes at 37°C under agitation. The cell suspension was filtered successively through 100-, 70- and 40-µm sterile nylon cell strainers (BD Biosciences, Le pont de Claix, France). Mononuclear cells were isolated from the cell suspension by Ficoll gradient centrifugation using Lymphocyte Separation Medium (PAA, Les Mureaux, France). dM were purified by positive selection using anti-CD14 magnetic beads (Miltenyi, Paris, France). Their purity was checked by flow cytometry and was 93% ± 3.8% (mean + SEM). Contaminating cells were mainly $CD45^{-}$ cells. dM were cultured at 2x106 cells/mL in HamF12 and DMEM Glutamax (Gibco, Cergy Pontoise, France) supplemented with 15% fetal calf serum (PAA), penicillin (0.1 U/mL) and streptomycin (10-8 g/L). dM were stimulated for 3 or 7 days prior to various assays with R848 at 5 µg/ml for TLR7/8 activation (Invivogen, Toulouse, France) and with IFN-γ at 100 ng/ml for polarization switch studies (R&D, Lille, France).

HIV-1 isolates and infection

For single-round infection, we used HIV-1 particles containing the luc reporter gene and pseudotyped with the vesicular stomatitis virus G protein (HIV-1/VSV-G). HIV1/ VSV-G was produced by transient cotransfection of HEK293T cells with proviral pNL4-3 Nef^{-} Env^{-} Luc^{+} DNA and the pMD2 VSV-G expression vector. Supernatants containing pseudotyped viruses were harvested 72 h after transfection, passed through 0.45-nm pore-size filters and stored at - 80°C. The viral stocks were titrated on HeLa P4P cells. dM were spinoculated with the HIV-1/VSV-G pseudotype (600 ng of p24 Ag/10^6 cells) for 30 minutes at 1200 g then incubated at 37°C for 30

minutes. The efficiency of infection by the viral pseudotype was determined 72h later by luciferase assay in cell lysates, using the Luciferase reagent (Promega, Lyon, France) on a Glomax luminometer, according to the manufacturer's instructions. For productive infection, HIV-1_{BaL} was used. HIV-1_{BaL} was amplified for 11 days in PHA-stimulated PBMC depleted of $CD8^+$ cells, from three blood donors. The virus was concentrated by centrifugation on Vivaspin 100 000-Kda columns (Sartorius, Palaiseau, France) at 2000 g for 30 minutes, and was titrated on PBMC. dM were incubated for 1 hour with HIV-1_{BaL} at 10^{-3} MOI at 37°C. Culture supernatants were collected every 3 or 4 days and stored at -80°C. HIV-1BaL production was measured by ELISA (Zeptometrix, Franklin, Massachusetts, USA) measurement of the viral core antigen p24 (p24 Ag) in culture supernatants, according to the manufacturer's instructions.

Decidual explants

Decidual tissues were cut into 0.3 cm^2 pieces. For flow cytometry, explants were placed on collagen sponge gels (Pfizer, Paris, France) in 1.5 ml of medium/well/sponge/piece prior to stimulation with R848 or IFN-γ. The decidual tissue and sponge were then minced and digested with 1 mg/mL collagenase IV (Sigma, St Quentin Fallavier, France) and 250 U/mL recombinant DNase I (Roche, Meylan, France) for 20 minutes at 37°C under agitation. The cell suspension was filtered through 40-µm sterile nylon cell strainers (BD Biosciences, Le pont de Claix, France). The total cell population was used for flow cytometry. Explants were stimulated overnight with R848 then infected with HIV-1_{BaL} for 12h. After several washes, explants were placed on collagen sponge gels. Experiments were all performed in triplicate and the mean values are reported in the figures.

Flow cytometry of cell surface markers

Adherent dM were washed with cold EDTA/PBS (2 mM) and detached from the plastic plates by pipetting without scraping. Cells were labeled with anti-CCR5 (APC-Cy7,clone 2D7, BD), anti-CD14 (Pacific Blue, clone 3.9, BD), anti-CD163 (PE, clone GHI/61, BD), anti-CD206 (APC, clone 19.2, BD), anti-CD4 (PE-Cy7, clone SK3, BD), anti-CD45 (Amcyan, clone 2D1, BD), anti-CD64 (FITC, clone 10.1, BD), anti-CD80 (PE, clone 307/4, BD), anti-CD86 (PE, clone 2331, BD), and anti-DC-SIGN (PE, clone 120507, R&D) (R&D, Lille, France). dM were incubated with an FcR blocking reagent (Miltenyi, Paris, France) before staining with the conjugated antibodies for 20 minutes at 4°C. After two EDTA/PBS washes, cells were fixed in 1% paraformaldehyde, and surface marker expression was determined with an LSRII 2-Blue 2-Violet 3-Red 5-Yelgr-laser configuration (BD Biosciences, Le pont de Claix, France). The results were analyzed with FlowJo 9.1.3. software (Tristar, Ashland, USA). MFI (%) was calculated as the ratio of treated dM (IFN-γ) or R848-treated dM to the unstimulated dM control.

Western blotting

Freshly isolated dM or dM cultured in 48-well plates were washed with PBS then lysed in 120 µL of lysis buffer (50 mM Tris·HCl, pH 7.4, 150 mM NaCl, 1 mM EDTA, and 1% TritonX-100) containing a protease and phosphatase inhibitor mixture (Roche, Meylan, France). Cell extracts (10–25 µg) were hybridized with the primary antibodies, followed by secondary horseradish peroxidase anti-mouse (Cell Signaling, Leiden, Netherlands) or anti-rabbit (Sigma-Aldrich, Saint Louis, USA) antibodies. Proteins were revealed on Hyperfilms (Amersham, Velizy-Villacoublay,

France) by using the Pierce ECL western blotting substrate (Thermo Scientific, Waltham, USA). The following primary antibodies were used: anti-p21 (clone CP74, Merck Millipore, Fontenay sous Bois, France), anti-IRF5 (ab140593, abcam, Paris, France) and anti-β-actin (clone AC-74, Sigma-Aldrich, Saint Louis, USA). Primary antibodies were all used at 1 :2000 dilution in 1% skimmed milk in PBS-0.05% Tween, except for anti-b-actin (1 :10 000).

The protein band intensity was quantified with the Image J software 1,47V and normalized to the actin band. Ratios (protein / actin) were then compared between the different conditions. Fold changes of IRF5 and p21 expression were calculated by comparing the normalized value of IRF5 and p21 from the IFN-γ-treated samples to the normalized value of IRF5 and p21 from the dM (US) control from the same donor.

HIV-1 DNA quantitative PCR (qPCR)

Total DNA in HIV-1/VSV-G-infected dM was extracted 72 h postinfection (p.i.) by using the DNeasy kit as recommended by the manufacturer (Qiagen, California, USA). Quantitative real-time PCR analysis of late (U5GAG) forms of viral DNA was carried on an ABI Prism 7500 sequence detection system as previously described [19]. Standards for U5GAG amplification products were generated by serial dilution of DNA extracted from HIV-1 8E5 cells containing one integrated copy of HIV-1 per cell. Integrated HIV-1 DNA was quantified by real-time Alu-LTR nested PCR using primers and probes described elsewhere, with some modifications [19]. Briefly, the first round of amplification was performed on a GeneAmp PCR system 9700 (Applied Biosystems, Saint Aubin, France). Integrated HIV-1 sequences were amplified by using the Expand High Fidelity kit (Roche, Meylan, France), two Alu primers (Alu F and Alu R)

and an LTR primer extended with an artificial tag sequence at the 5' end of the oligonucleotide (NY1R). Real-time nested PCR was run on the ABI Prism 7500 system using a 1/10 dilution of the first-round PCR product as template (primers NY2F and NY2R; probe NY2Alu). The integrated HIV-1 DNA copy number was determined with reference to a standard curve generated by concurrent amplification of HeLa R7 Neo cell DNA. A nested PCR conducted in parallel without the Alu primers in the first round gave a very weak background signal. The number of integrated HIV-1 DNA copies was obtained by subtracting the copy number measured without the Alu primers in the first round from the copy number measured in the full reaction. The amount of viral DNA was normalized to the endogenous reference albumin gene (for total DNA extracts). Standard curves were generated by serial dilution of a commercial human genomic DNA (Roche, Meylan, France).

Supplementary Figure S1

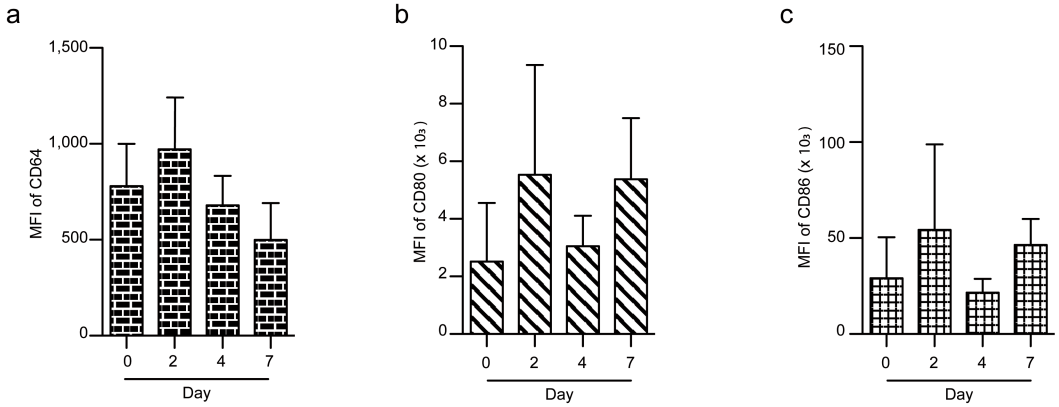

Supplementary Figure S2

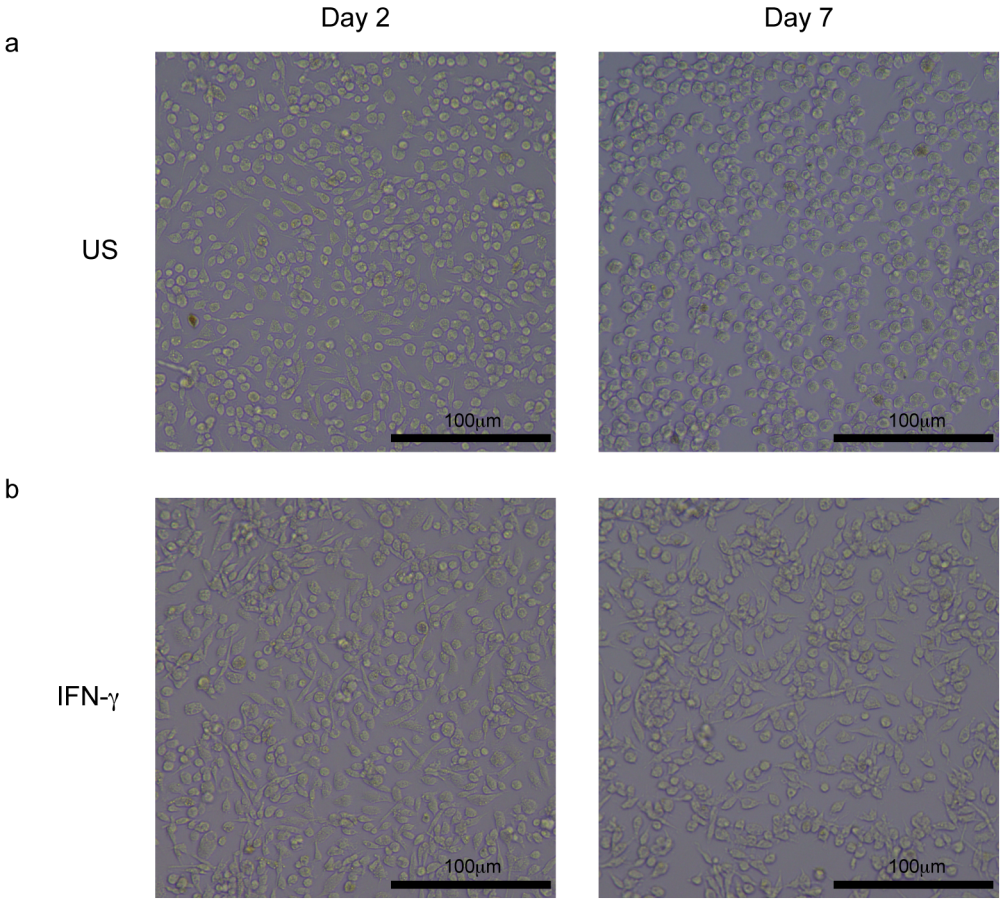

Supplementary Figure S3

a

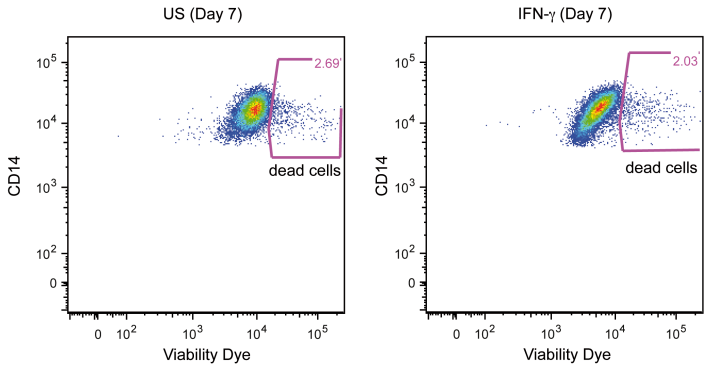
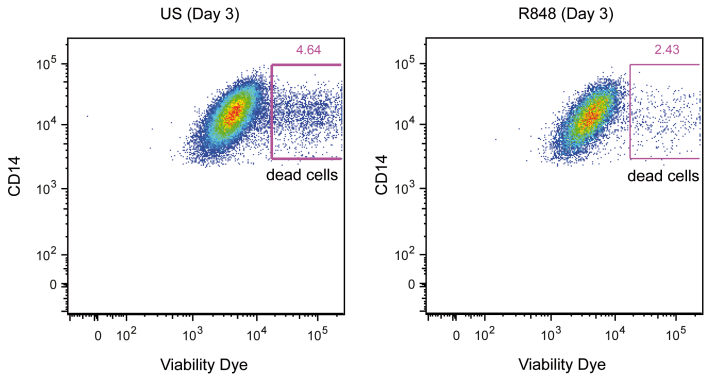
b